13th ANKARA INTERNATIONAL AEROSPACE CONFERENCE
17-19 September 2025 - METU, Ankara TURKIYE

AIAC-2025-143

ADAPTIVE MEASUREMENT ERROR COVARIANCE ADJUSTMENT FOR VISION-AIDED SPACECRAFT NAVIGATION

Abdurrahim Muratoglu[1,2,3,*], H. Ersin Söken[1,†] and Ozan Tekinalp[1,‡]
[1]Middle East Technical University, Ankara, Türkiye
[2]University of Stuttgart, Stuttgart, Germany
[3]Turkish-German University, Istanbul, Türkiye

ABSTRACT

This paper introduces an adaptive method for spacecraft navigation that dynamically adjusts Kalman Filter parameters using Cramér-Rao Lower Bound analysis. While line-of-sight based visual observations of celestial bodies yield valuable positional references that enhance filter-based solutions for interplanetary navigation, their accuracy varies with the ranges to observed bodies and the angular separation between these observations. Our approach quantifies theoretical lower error variance limits for each observation scenario throughout a trajectory, enabling more precise and reliable specification of measurement covariance matrices. Simulation results, validated through Monte Carlo analysis, demonstrate improved position and velocity estimation accuracy throughout translunar trajectories, particularly during geometrically challenging segments where conventional range based methods struggle to maintain consistent estimation performance.

Keywords: vision-aided navigation; autonomous navigation; celestial observation; bearing; position estimation; triangulation; Kalman filter; Cramér-Rao Lower Bound

INTRODUCTION

Space exploration missions demand reliable navigation estimation systems for successful operations, ensuring precise positioning, guidance, and autonomy in challenging trajectories and mission phases [Pöhlmann et al., 2023]. As spacecraft journey deeper into space, the development of autonomous navigation capabilities becomes essential for improving mission resilience and minimizing operational expenses. These capabilities enable higher levels of autonomy, particularly since the significant light-time delays render Earth-based real-time control impractical during key mission operations [Starek et al., 2016]. Conventional spacecraft navigation approaches depend heavily on precise initial state determination and the continuous integration of Inertial Measurement Unit (IMU) sensor data, creating a foundation for position and velocity estimation throughout the mission trajectory. However, these approaches suffer from accumulated errors over time, limiting their long-term reliability. Various environmental factors, including gravitational perturbations and unknown gravity fields of celestial bodies, further contribute to this uncertainty [Trawny et al., 2007].

Vision-aided navigation systems have emerged as promising solutions to overcome these limitations. By uti-

*GRA in Aerospace Engineering Department, Email: moglu@metu.edu.tr
†Assoc. Prof. in Aerospace Engineering Department, Email: esoken@metu.edu.tr
‡Prof. in Aerospace Engineering Department, Email: tekinalp@metu.edu.tr

lizing information acquired from optical sensors, these systems can provide absolute position measurements that complement IMU data providing more accurate pose estimations [Alkendi et al., 2021]. Among various vision-based techniques, Line-of-Sight (LoS) navigation (also referred as angles-only navigation) by using the measurements of celestial bodies such as planets, moons, and asteroids, offer particularly valuable navigation references throughout interplanetary trajectories [Kaplan, 2011; Franzese et al., 2021; Henry and Christian, 2023; Muratoglu et al., 2025b]. The mathematical foundation for LoS navigation lies in triangulation techniques, which uses these unit LoS vectors towards celestial bodies with known ephemeris data to geometrically estimate the position and velocity of spacecraft. Although this approach has been proven to be effective across various mission scenarios, a fundamental challenge persists in establishing the optimal balance between the spacecraft's mathematical orbital model and the integration of measurement updates within state estimation filters.

A critical limitation of current approaches is the difficulty in specifying appropriate measurement accuracy parameters in filter tuning for triangulation with LoS measurements. The geometric configuration between the spacecraft and observed celestial bodies significantly influences triangulation performance, with accuracy degrading when observation geometries approach collinearity or when the relative ranges to the observed objects increased. This variable accuracy presents challenges for consistent filter performance throughout different trajectory phases.

In this work, we propose a novel method for dynamically adjusting filter parameters by leveraging a recently developed Cramér-Rao Lower Bound (CRLB) based geometric performance metric [Muratoglu et al., 2025a]. This approach provides theoretical error limits for different observation configurations, enabling more precise specification of measurement covariance matrices in Kalman filters. By establishing a better equilibrium between mathematical models and measurement updates, our method enhances overall navigation accuracy and reliability throughout interplanetary trajectories.

The proposed adaptive technique will be beneficial for vision-aided spacecraft navigation in deep space missions that employ celestial triangulation, where observation geometries tend to have continuous evolution and may possibly encounter extreme configurations. These geometric extremities can potentially degrade triangulation accuracy and may compromise filter performance when tuning approaches based on fixed-parameter or relative distances to the observed objects are employed. The dynamic covariance adjustment capability based on CRLB-based figure of merit is designed to address these challenges by adapting to the varying measurement reliability that occurs throughout the mission profile.

METHODS

Triangulation

Celestial triangulation enables position estimation through LoS observations of two or more celestial bodies and their known ephemeris information. This represents the resection case of triangulation, where the positions of two vertices are known, and the third vertex of the observer to be determined from angular measurements. As illustrated in Figure 1, the spacecraft at position $\boldsymbol{P}_0$ observes two celestial bodies at positions $\boldsymbol{P}_1$ and $\boldsymbol{P}_2$, with unit LoS vectors $\boldsymbol{r}_{01}$ and $\boldsymbol{r}_{02}$ pointing from the spacecraft towards these bodies, respectively, while the relative position vector from the first to the second body, $\boldsymbol{R}_{12}$, is known via ephemerides. The relation for obtaining the relative position vector from the observer to the 1^{st} body is formularized by implementing the law of sines as:

$$\boldsymbol{R}_{01} = \frac{\|\boldsymbol{R}_{12} \times \boldsymbol{r}_{02}\|}{\|\boldsymbol{r}_{01} \times \boldsymbol{r}_{02}\|}\boldsymbol{r}_{01} \tag{1}$$

$$\boldsymbol{R}_{02} = \frac{\|\boldsymbol{R}_{12} \times \boldsymbol{r}_{01}\|}{\|\boldsymbol{r}_{01} \times \boldsymbol{r}_{02}\|}\boldsymbol{r}_{02} \tag{2}$$

Error Model

The accuracy of triangulation based position estimation is fundamentally limited by errors in the LoS vector measurements. These errors arise from various sources including sensor noise, attitude determination uncertainties, and celestial body centroiding inaccuracies. While planetary ephemeris uncertainties of observed bodies represent an additional error source, these are predetermined by ground based orbit determination

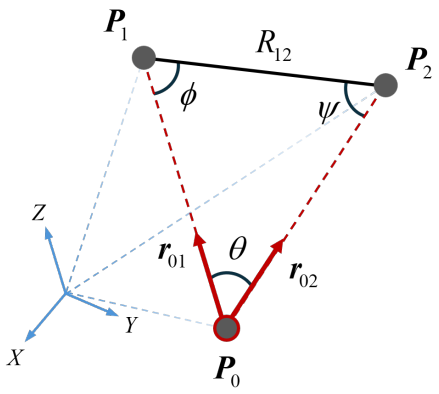

Figure 1: Triangulation formed by two observed objects with known locations (via ephemeris) with respect to the inertial reference frame (ECI)

models to be utilized onboard and cannot be influenced by onboard sensing systems. It should be noted that the position of the Moon with respect to Earth is known with submeter accuracy, while the positions of inner planets are estimated with subkilometer accuracy [Folkner et al., 2014]. Thus, these ephemeris errors will not be considered within the estimation process. Therefore, the focus is placed on modeling the LoS measurement uncertainties. To quantify the impact of these errors on navigation performance, a statistical error model is essential. The measured unit LoS vector towards observed i^{th} body, $\tilde{\boldsymbol{r}}_{0i}$ incorporates additive noise while maintaining vectorial unit magnitude, deviating from the true unit LoS vector $\boldsymbol{r}_{0i}$ through a noise component $\boldsymbol{\omega}_{0i}$.

$$\tilde{\boldsymbol{r}}_{0i} = \frac{\boldsymbol{r}_{0i} + \boldsymbol{\omega}_{0i}}{\|\boldsymbol{r}_{0i} + \boldsymbol{\omega}_{0i}\|} \tag{3}$$

where the noise component has a zero-mean normal distribution with an error covariance according to Quest Measurement Model (QMM).

$$\boldsymbol{\omega}_{0i} \sim \mathcal{N}\left(\mathbf{0}_{3\times 1}, \mathbf{R}_{\text{QMM}}\right) \tag{4}$$

The error covariance matrix $\mathbf{R}_{\text{QMM}}$ with isotropic direction uncertainty is given as [Shuster and Oh, 1981]:

$$\mathbf{R}_{\text{QMM}} = \mathbb{E}\left[\boldsymbol{\omega}_{0i}\boldsymbol{\omega}_{0i}^{\top}\right] = \sigma_i^2\left(\mathbf{I}_{3\times 3} - \boldsymbol{r}_{0i}\boldsymbol{r}_{0i}^{\top}\right) \tag{5}$$

where σ_i denotes the standard deviation of the pointing errors in i^{th} unit LoS measurements, and $\mathbf{I}_{3\times 3}$ the identity matrix of size (3×3).

Cramér-Rao Lower Bound Based Performance Metric for Measurements

The Cramér-Rao Lower Bound (CRLB) is a fundamental theorem in estimation theory that establishes the achievable theoretical minimum error limit for an unbiased estimator. This framework provides valuable insights into the quality of estimations derived from noisy measurements. This theoretical limit is mathematically defined through the inverse of the Fisher Information Matrix, $\mathbf{F}$, which quantifies how measurement sensitivity relates to the estimated parameters. When applied to celestial triangulation problems, the CRLB framework reveals how measurement errors and geometric factors constrain the precision of position estimates. In this sense, the theoretical bounds provided by CRLB analysis serve as a valuable benchmark for evaluating the measurement quality and guiding the development of adaptive filter strategies that dynamically respond to varying observation conditions throughout the mission trajectory.

In the presence of LoS measurement noise, different triangulation geometries yield position estimates with varying accuracies. The CRLB technique can quantify these theoretical accuracy limits, providing a performance metric that accounts for both measurement uncertainties and geometric configurations including the angular separation of LoS vectors and the relative distances between observer and observed bodies. In case of two-body observation, the CRLB asserts that the estimation error covariance of an unbiased estimator cannot be smaller than the inverse of $\mathbf{F}$ [Bar-Shalom et al., 2001; Crassidis and Junkins, 2011]:

$$\mathbb{E}\left[\left[\hat{\boldsymbol{P}}_0 - \boldsymbol{P}_0\right]\left[\hat{\boldsymbol{P}}_0 - \boldsymbol{P}_0\right]^T\right] \geq \mathbf{F}^{-1} \tag{6}$$

where $\hat{\boldsymbol{P}}_0$ and $\boldsymbol{P}_0$ are the estimated and real spacecraft positions and the $\mathbf{F}$ matrix is given [Muratoglu et al., 2025a] as:

$$\mathbf{F} = \sum_{i=1}^{n} \frac{1}{\sigma_i^2 R_{0i}^2}\left(\mathbf{I}_{3\times 3} - \boldsymbol{r}_{0i}\boldsymbol{r}_{0i}^\top\right) \tag{7}$$

where σ_i denotes the measurement error standard deviation, R_{0i} the range between observer and observed i^{th} body, and $\boldsymbol{r}_{0i}$ the unit LoS vector towards the i^{th} body. Then, the theoretical lower error variance limit on the observer location by the triangulation estimation is computed by [Muratoglu et al., 2025a]:

$$\Sigma\left(\boldsymbol{P}_0\right) = \frac{1}{2}\text{Tr}\left(\mathbf{F}^{-1}\right) \tag{8}$$

In practical applications, the true LoS vectors $\boldsymbol{r}_{0i}$ are not directly available, instead only the noisy measurements $\tilde{\boldsymbol{r}}_{0i}$ can be observed. Substituting the measured vectors in place of the true vectors makes the covariance matrix approximately correct. However, as true values are inherently unavailable in practice, this approximation becomes inevitable to be made and leads only second-order effects [Shuster, 1990; Cheng et al., 2006]. Furthermore, since the $\mathbf{F}$ matrix is primarily used for relative performance assessment and filter tuning rather than absolute accuracy prediction, this practical approximation provides reliable guidance for adaptive measurement covariance adjustment throughout the mission trajectory.

Extended Kalman Filter

The Extended Kalman Filter (EKF) is used for spacecraft position estimation since it is suitable for orbital space applications, provided that the system dynamic model and measurements are correctly characterized [Erkeç and Hajiyev, 2022]. The EKF accommodates the nonlinear nature of orbital dynamics, unlike linear filtering approaches. Even though it considers nonlinearities of orbital dynamics, nonlinearities and uncertainties in measurements can cause degradation in EKF performance. Thus, the measurement covariance matrix must be accurately specified to achieve optimal navigation estimation performance. When uncertainties in measurements are improperly characterized, the filter may either overdepend on noisy measurements or underutilize valuable observational information, leading to suboptimal state estimates. This becomes particularly pronounced in LoS based vision-aided navigation systems where measurement accuracy varies significantly with changing geometric configurations throughout the trajectory, necessitating adaptive approaches to maintain consistent estimation performance.

The state vector of the spacecraft is defined as a 6×1 dimensional vector containing position and velocity components in the Earth Centered Inertial (ECI) frame of reference:

$$\mathbf{x} = \left[x, y, z, \dot{x}, \dot{y}, \dot{z}\right]^\top \tag{9}$$

where x, y, and z represent the spacecraft position coordinates and $\dot{x}$, $\dot{y}$, and $\dot{z}$ denote the corresponding velocity components. The process model describes the trajectory dynamics through the nonlinear state transition function as:

$$\mathbf{x}_k = \mathbf{f}\left(\mathbf{x}_{k-1}, \mathbf{u}_k\right) + \mathbf{v}_k \tag{10}$$

where $\mathbf{f}\left(\mathbf{x}_{k-1}\right)$ denotes the nonlinear dynamics incorporating the gravitational forces (3-body) acting on the spacecraft, and $\mathbf{v}_{k-1}$ denotes the process noise accounting for unmodeled dynamics and modeling uncertainties with covariance matrix $\mathbf{Q}$ which is specified by:

$$\mathbf{Q} = \begin{bmatrix} \frac{1}{3}\Delta t^3 \mathbf{I}_{3\times 3} & \mathbf{0}_{3\times 3} \\ \mathbf{0}_{3\times 3} & \Delta t \mathbf{I}_{3\times 3} \end{bmatrix} q \tag{11}$$

where q is the spectral noise density [Stacey and D'Amico, 2021]. The measurement model describes the spacecraft state to triangulation-based measurement via LoS observations toward celestial bodies:

$$\tilde{\mathbf{y}}_k = \mathbf{h}\left(\mathbf{x}_k\right) + \mathbf{w}_k \tag{12}$$

where $\mathbf{h}(\mathbf{x}_k)$ is nonlinear observation function, and $\mathbf{w}_k$ represents the measurement noise with covariance matrix $\mathbf{R}_k$ which is adaptively adjusted throughout the trajectory.

To demonstrate the effectiveness of the proposed CRLB-based approach, it is compared against a conventional distance-based method for $\mathbf{R}_k$ specification. With the distance-based method, one of the best approaches is to average the error variances of observations to determine the $\mathbf{R}_k$, as the distance to an observed body increases, small angular measurement errors translate into proportionally larger position uncertainties, following a linear relationship with range. Accordingly, the measurement noise covariance matrix is formulated by weighting the individual error variances in observations:

$$\mathbf{R}_k = \left(\frac{1}{n} \sum_{i=1}^{n} \sigma_i^2 \tilde{R}_{0i}^2 \right) \mathbf{I}_{3\times 3} \tag{13}$$

where n is the number of observed celestial bodies, σ_i is the error standard deviation in i^{th} LoS observation, and $\tilde{R}_{0i}$ denotes the measured range from the spacecraft to the i^{th} body. While this approach accounts for the degradation of measurement accuracy with increasing noise and distances to celestial bodies, it fails to capture the complete geometric picture of triangulation performance, particularly the critical impact of angular separation between LoS vectors on estimation accuracy.

On the other side, the CRLB-based adjustment enables the filter to maintain performance by appropriately weighting the measurement updates according to the theoretical accuracy limits imposed by both range and angular observation conditions.

$$\mathbf{R}_k = \Sigma_k \mathbf{I}_{3\times 3} \tag{14}$$

where Σ_k denotes the calculated CRLB value (see Eqn.8) for the spacecraft position at the corresponding time step with $\mathbf{F}$ as:

$$\mathbf{F} = \sum_{i=1}^{n} \frac{1}{\sigma_i^2 \tilde{R}_{0i}^2} \left(\mathbf{I}_{3\times 3} - \tilde{\boldsymbol{r}}_{0i} \tilde{\boldsymbol{r}}_{0i}^{\top} \right) \tag{15}$$

where $\tilde{\boldsymbol{r}}_{0i}$ represents the measured unit LoS vector towards the i^{th} body. This adaptive adjustment enables the filter to maintain performance by appropriately weighting the measurement updates according to the theoretical accuracy limits imposed by the observation conditions.

RESULTS AND DISCUSSION

The effectiveness of the proposed adaptive measurement covariance adjustment method was assessed via numerical simulations conducted along the translunar trajectory described in previous work [Muratoglu et al., 2025b]. The spacecraft departed from a 400 km circular Earth orbit and traveled to a 100 km lunar orbit over approximately 3.35 days. The simulations were performed with a time step of $\Delta t = 30$ s, and at each time step along the trajectory, LoS measurements towards Earth and Moon were obtained and corrupted with noise following the described error model with a standard deviation of $\sigma = 0.001$ rad. The process noise power spectral density, q was set to 10^{-6} within process noise covariance matrix $\mathbf{Q}$ to present unmodeled dynamics and modeling uncertainties. The measurement noise covariance matrix $\mathbf{R}$ was updated at each step of the simulation, based on the calculated CRLB value.

To provide statistical validation of performance improvements and verify the consistency of the filter uncertainty estimates, Monte Carlo simulations of 200 independent runs were performed. Each run utilized identical trajectory dynamics but incorporated different realizations of measurement noise generated according to the error model described previously. The initial state estimates for the filter were perturbed from the true initial conditions to simulate realistic initialization uncertainties, with position estimates obtained by rotating the true initial position vector through random angles with LoS measurement uncertainty $\sigma = 0.001$ rad, and velocity estimates perturbed with half the proportional magnitude 0.5σ. These perturbations were independently randomized for each Monte Carlo run. This statistical analysis framework enables the assessment of both the mean performance and consistency of the proposed adaptive CRLB-based method compared to the adaptive distance-based approach.

Figure 2 illustrates the evolution of key geometric parameters and the corresponding CRLB-based performance metric throughout the mission trajectory. The change in ranges from the spacecraft to Earth and Moon

during the translunar transfer is shown in the upper part. The angular separation between LoS vectors exhibits challenging phases where they approach collinearity, particularly during the initial departure phase. The CRLB-based error variance metric captures the effect of both range and angular variations, revealing that the triangulation measurement accuracy and consequently position estimation accuracy depend on the interaction between these factors rather than individual range measurements alone.

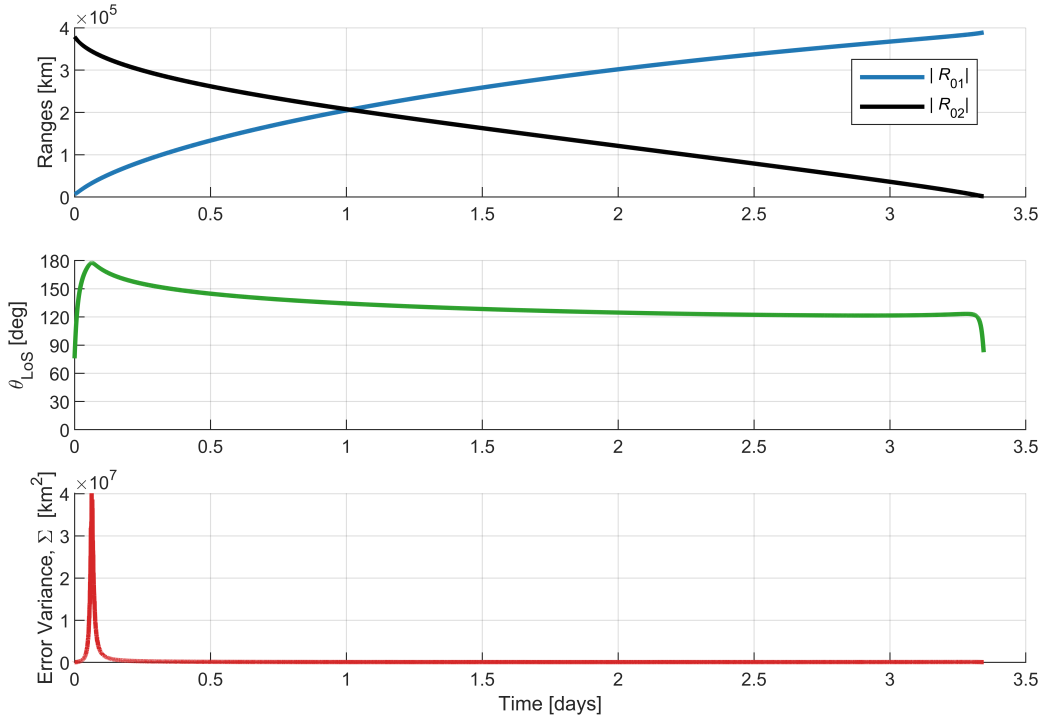

Figure 2: Evolution of triangulation geometry and performance metric along the trajectory: ranges to observed bodies (*top*), angular separation (*middle*), and CRLB-based error variance (*bottom*)

Figure 3 presents the position and velocity estimation errors for a representative single simulation run, comparing the distance-based measurement covariance approach with the adaptive CRLB-based adjustment strategy. The relative distance-based approach, which adjusts measurement uncertainty parameters according to average of range-weighted measurement variances, exhibits notable performance degradation during specific trajectory segments especially between $t = 0$ and $t = 0.5$ days where the angles between the LoS vectors approach to 180°. While this method accounts for changing ranges to the observed bodies, it fails to capture the full geometric complexity of the triangulation problem. This limitation manifests as error spikes that temporarily exceed the 3σ confidence bounds, indicating that the uncertainty representation of the filter becomes inconsistent with the actual estimation performance. The method's inability to account for overall angular geometry results in overconfident estimates during low accuracy measurement phases.

In contrast, the adaptive CRLB-based approach demonstrates lower estimation errors with improved error containment throughout the trajectory. By dynamically adjusting the measurement covariance matrix $\mathbf{R}$ according to the comprehensive geometric performance metric, which considers both relative distances and angular separations between LoS vectors and provides theoretical error variance border, the filter maintains consistent estimation accuracy even during geometrically challenging configurations. The most significant improvement appears when the triangulation geometry approaches near-collinear configurations, where distance-based methods alone cannot adequately represent the degraded measurement quality. During these phases, the CRLB-based approach appropriately increases the measurement covariance, preventing the filter from over-relying on less reliable measurements and maintaining estimation performance.

The velocity estimation results show similar characteristics to the position estimates, with the CRLB-based adaptive method providing more stable estimates and better uncertainty quantification. The error bounds accurately reflect the actual error magnitudes throughout the trajectory, with estimation errors remaining within the predicted 3σ boundaries. This indicates that the theoretical CRLB-based analysis effectively captures the

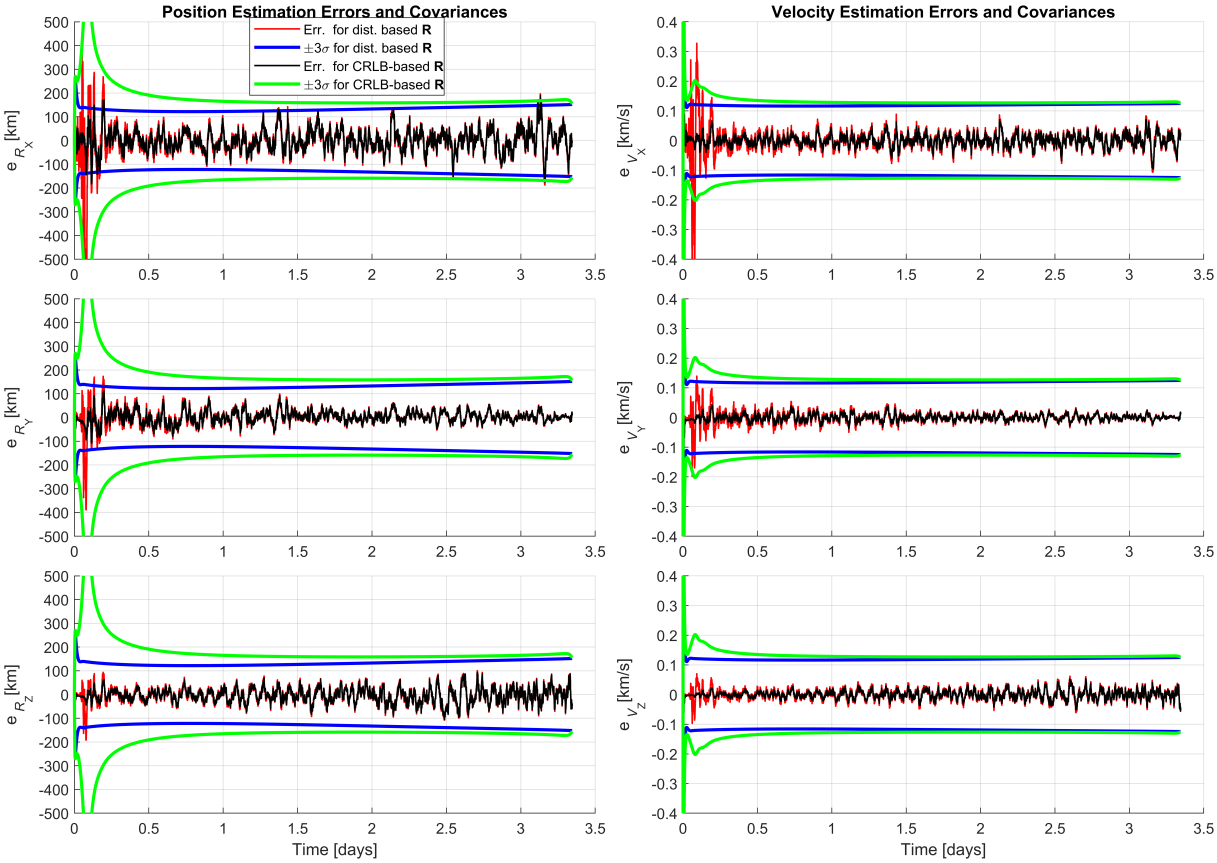

Figure 3: Comparison of EKF position and velocity estimation errors using distance-based versus CRLB-based adaptive measurement covariance adjustment with corresponding 3σ uncertainty boundaries (single-run)

actual measurement uncertainty variations encountered during the mission, providing more reliable guidance for filter tuning.

While this single-run simulation result demonstrates the characteristic behavior of both methods, statistical validation across multiple noise realizations is needed to confirm the consistency of these performance differences. Figure 4 presents the mean position and velocity estimation errors averaged across all Monte Carlo runs, along with the corresponding mean 3σ uncertainty boundaries for both methods. The mean error results confirm the systematic performance advantage of the CRLB-based approach observed in the single-run analysis. The CRLB-based method maintains smaller mean errors throughout the trajectory, particularly during intervals where the triangulation geometry approaches ill-conditioned configurations. Similarly, Figure 5 presents the root-mean-square (RMS) errors for position and velocity computed from all Monte Carlo runs, providing a measure of the overall estimation accuracy for both methods. Quantitative comparison reveals that the CRLB-based adaptive method reduces peak position RMS errors by approximately 58.8% and peak velocity RMS errors by approximately 66.5% relative to the conventional distance-based approach, demonstrating significant improvement in estimation accuracy during the most challenging trajectory segments. Beyond these peak improvements, there are consistent advantages throughout the entire trajectory, achieving an overall position error reduction of approximately 12.8% and velocity error reduction of approximately 30% when averaged across the complete trajectory.

These findings validate that incorporating comprehensive geometric performance metrics into filter design enables more robust navigation solutions for interplanetary missions, where observation geometries continuously evolve. The adaptive capability becomes particularly valuable during extended mission phases where the conventional tuning approaches may become inadequate due to dynamic nature of geometric configurations and their varying impact on measurement reliability. This approach shows potential for extension to multi-body observation scenarios where the geometric complexity increases even further.

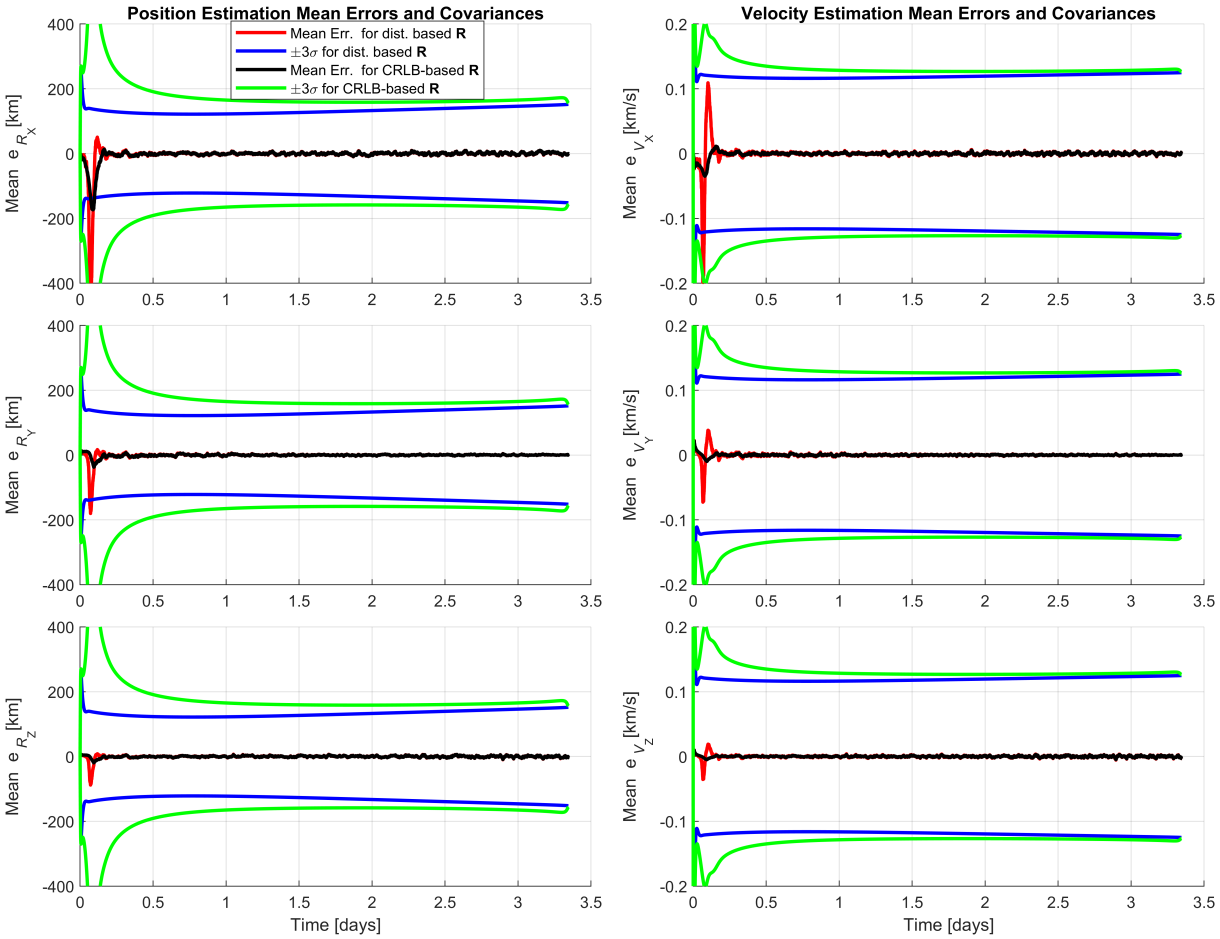

Figure 4: Mean position and velocity estimation errors from Monte Carlo simulations (200 runs) comparing distance-based versus CRLB-based adaptive measurement covariance adjustment methods with corresponding mean 3σ uncertainty boundaries

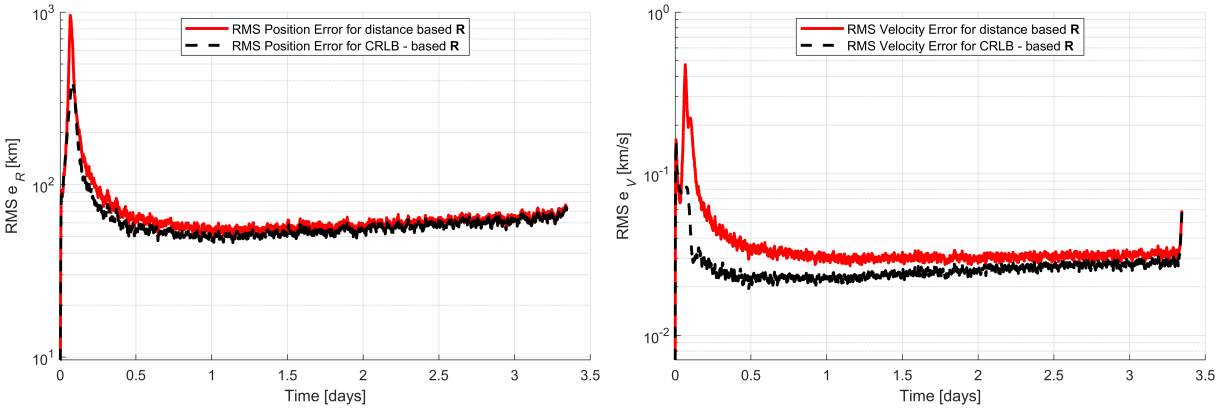

Figure 5: Root-mean-square (RMS) position and velocity errors (logarithmic scale) from Monte Carlo simulations (200 runs) comparing the overall estimation accuracy of distance-based and CRLB-based adaptive measurement covariance adjustment methods

CONCLUSIONS

This study presented an adaptive measurement error covariance adjustment method for vision-aided spacecraft navigation that leverages CRLB analysis to dynamically optimize the performance of Kalman filter (EKF). The proposed approach addresses the fundamental challenge in celestial triangulation where measurement accuracy varies significantly with geometric configurations including both angular separation of observations and relative distances to those bodies. The adaptive CRLB-based method demonstrated improved performance compared to conventional distance-based approaches throughout translunar trajectory simulations, validated through Monte Carlo analysis of 200 independent runs. The technique maintained consistent estimation accuracy during geometrically challenging phases, particularly when LoS vectors approached collinear configurations where traditional methods experienced significant performance degradation due to excessive degradation in measurement accuracy. Position and velocity estimation errors were effectively contained within theoretical 3σ boundaries, validating the CRLB-based performance metric. The dynamic adjustment of measurement covariance matrices based on comprehensive geometric performance metrics enabled more robust state estimation throughout the mission profile. By establishing optimal equilibrium between mathematical orbital models and measurement updates, this method enhances navigation reliability for interplanetary missions that implement onboard optical navigation.

Acknowledgments

A. Muratoglu thanks TUBITAK 2214-A International Doctoral Research Fellowship Programme for supporting his researches at Institute for Photogrammetry and Geoinformatics, University of Stuttgart. This work was carried out as a part of the Ph.D. thesis in Aerospace Engineering at Middle East Technical University by A. Muratoglu under the supervision of H. E. Söken.

References

Alkendi, Y., Seneviratne, L., and Zweiri, Y. (2021). State of the art in vision-based localization techniques for autonomous navigation systems. *IEEE Access*, 9:76847–76874.

Bar-Shalom, Y., Li, X. R., and Kirubarajan, T. (2001). *Estimation with applications to tracking and navigation*. John Wiley & Sons, Hoboken, NJ, USA.

Cheng, Y., Crassidis, J. L., and Markley, F. L. (2006). Attitude estimation for large field-of-view sensors. *The Journal of the Astronautical Sciences*, 54(3):433–448.

Crassidis, J. L. and Junkins, J. L. (2011). *Optimal estimation of dynamic systems, second edition*. Chapman & Hall/CRC, Boca Raton, FL, USA, 2 edition.

Erkeç, T. Y. and Hajiyev, C. (2022). Formation flight for close satellites with gps-based state estimation method. *IEEE Sensors Journal*, 22(15):15457–15464.

Folkner, W. M., Williams, J. G., Boggs, D. H., Park, R. S., and Kuchynka, P. (2014). The planetary and lunar ephemerides de430 and de431. *Interplanetary network progress report*, 196(1):42–196.

Franzese, V., Topputo, F., Ankersen, F., and Walker, R. (2021). Deep-space optical navigation for m-argo mission. *The Journal of the Astronautical Sciences*, 68:1034–1055.

Henry, S. and Christian, J. A. (2023). Absolute triangulation algorithms for space exploration. *Journal of Guidance, Control, and Dynamics*, 46(1):21–46.

Kaplan, G. H. (2011). Angles-only navigation: Position and velocity solution from absolute triangulation. *Navigation*, 58(3):187–201.

Muratoglu, A., Söken, H. E., and Soergel, U. (2025a). Error covariance analyses for celestial triangulation and its optimality: Improved linear optimal sine triangulation. *Aerospace*, 12(5):385.

Muratoglu, A., Söken, H. E., and Tekinalp, O. (2025b). Visual navigation for lunar missions using sequential triangulation technique. *Engineering Proceedings*, 90(1):27.

Pöhlmann, R., Staudinger, E., Zhang, S., Broghammer, F., Dammann, A., and Hoeher, P. A. (2023). Cooperative radio navigation for robotic exploration: Evaluation of a space-analogue mission. In *2023 IEEE/ION Position, Location and Navigation Symposium (PLANS)*, pages 372–380. IEEE.

Shuster, M. D. (1990). Kalman filtering of spacecraft attitude and the quest model. *Journal of the Astronautical Sciences*, 38(3):377–393.

Shuster, M. D. and Oh, S. D. (1981). Three-axis attitude determination from vector observations. *Journal of guidance and Control*, 4(1):70–77.

Stacey, N. and D'Amico, S. (2021). Adaptive and dynamically constrained process noise estimation for orbit determination. *IEEE Transactions on Aerospace and Electronic Systems*, 57(5):2920–2937.

Starek, J. A., Açıkmeşe, B., Nesnas, I. A., and Pavone, M. (2016). *Spacecraft Autonomy Challenges for Next-Generation Space Missions*, page 11. Springer Berlin Heidelberg, Berlin, Heidelberg.

Trawny, N., Mourikis, A. I., Roumeliotis, S. I., Johnson, A. E., and Montgomery, J. F. (2007). Vision-aided inertial navigation for pin-point landing using observations of mapped landmarks. *Journal of Field Robotics*, 24(5):357–378.